

Effects of Salvianolic Acid B/ginsenoside Rg1 Combination Against Chronic Pulmonary Embolism Induced by Polystyrene Microspheres

Huimiao BIAN¹, Na HAN¹, Linlin WANG, Xiaoyu WANG, Kenka CHO, Jun YIN, and Baohong JIANG

Accepted November 16, 2021

Published online December 21, 2021

Issue online December 23, 2021

Original article

BIAN H., HAN N., WANG L., WANG X., CHO K., YIN J., JIANG B. 2021. Effects of salvianolic acid B/ginsenoside Rg1 combination against chronic pulmonary embolism induced by polystyrene microspheres. *Folia Biologica (Kraków)* **69**: 189-198.

Pulmonary embolism (PE) is the most life-threatening complication of venous thromboembolism, but few effective treatments have been discovered to attenuate chronic PE currently. In this study, we investigated the protective effects of salvianolic acid B (SalB) and ginsenoside Rg1 (Rg1) combination (SalB/Rg1) on chronic PE and explored the potential mechanisms. The PE model was induced by 45 μ m polystyrene microspheres and 20 mg/kg of SalB/Rg1 was administered to PE rats intraperitoneally. A histopathological analysis of the lungs and heart was performed through hematoxylin and eosin staining and immunohistochemical analysis. The pulmonary index and right ventricular cardiomyocyte cross-sectional area were evaluated. SalB/Rg1 markedly downregulated pulmonary index, attenuated pulmonary interstitial changes, suppressed neutrophil infiltration, prevented collagen deposition, and inhibited MMP-9 activities in the lung. We also found that SalB/Rg1 improved right ventricular hypertrophy accompanied by reducing the cardiomyocyte cross-sectional area. These data suggest that SalB/Rg1 played a protective role against microsphere-induced PE and holds a high potential for the treatment of PE in the future.

Key words: salvianolic acid B, ginsenoside Rg1, pulmonary embolism, polystyrene microspheres.

Huimiao BIAN¹, Na HAN¹, Jun YIN[✉], School of Traditional Chinese Material, Shenyang Pharmaceutical University, Shenyang, China.

E-mail: yinjun826@sina.com

Huimiao BIAN, Linlin WANG, Xiaoyu WANG, Baohong JIANG[✉], Shanghai Institute of Materia Medica, Chinese Academy of Sciences, Shanghai, China.

E-mail: jiangbh@simm.ac.cn

Kenka CHO, Takarazuka University of Medical and Health Care, Hanayashiki-Midorigaoka, Takarazuka, Japan

¹These two authors share the first authorship

Abbreviations

CCSA: Cardiomyocyte cross-sectional area

HW/TL: Heart weight per tibial length

HR: Heart rate

HE: Hematoxylin and eosin

IOD: Integrated optical density

LPI: Left pulmonary index

MMPs: Matrix metalloproteinases

MMP-9: Matrix metalloproteinase-9

MMP-12: Matrix metalloproteinase-12

PE: Pulmonary embolism

PI: Pulmonary index

RPI: Right pulmonary index

RV: Right ventricular

RH/(LH+S): Ratio of right heart weight to left heart plus septum weight

Pulmonary embolism (PE) is a disease in which various emboli enter the pulmonary artery and prevent blood from flowing to the lungs. The annual morbidity of PE has revealed a rising tendency over time (WENDELBOE & RASKOB 2016; KONSTANTINIDES *et al.* 2019). PE is the third most common cardiovascular cause of death after myocardial infarction and stroke in China. PE patients still face the huge challenge of the deficiency of therapeutic medicines in clinic.

Chronic PE, in which residual clots in the pulmonary arteries continue to exist after acute PE, leads to pulmonary artery hypertension (BRESSER *et al.* 2004; NETO-NEVES *et al.* 2017). The current treatment for PE is focused on removing the mechanical obstruction through thrombolysis and anticoagulation. In certain cases, a surgical method, embolectomy, is also recommended (TOBA *et al.* 2008). The drug of thrombolysis includes recombinant tissue plasminogen activator (recombinant tPA), direct thrombin inhibitors, and factor Xa inhibitors (BARCO *et al.* 2020). Anticoagulation drugs include low-molecular-weight heparin and warfarin (YANG *et al.* 2020). These medical treatments are always used as a first aid and have been proved to improve survival. Symptoms of chronic PE included lung interstitial pathological changes, pulmonary inflammation, pulmonary fibrosis, and right ventricular (RV) hypertrophy.

Salvianolic acid B (SalB) and ginsenoside Rg1 (Rg1) are the representative active ingredients of *Salviae miltiorrhizae* and *Panax notoginseng*, respectively. Previous studies demonstrated the powerful effects of Rg1 against inflammation and fibrosis through various animal models (BAO *et al.* 2015). SalB was reported to hold antioxidant effects and prevent myocardial ischemia (QIAO & XU 2016). As the combination of SalB with Rg1, our previous studies have demonstrated that SalB/Rg1 held significant effects on cardio-protection with high safety (ZHAO *et al.* 2015; DENG *et al.* 2015a; DENG *et al.* 2015b). In the present study, we evaluate the effects of SalB/Rg1 on chronic PE.

Materials and Methods

Materials

56 healthy Wistar male rats (200–220 g) were purchased from the Shanghai Center of Experimental Animals, Chinese Academy of Sciences. All studies were approved by the Animal Care and Use Committee at the Shanghai Institute of Materia Medica (IACUC number: 2019-08-GDA-64). Polystyrene microspheres were purchased from Beijing Zhongke Thunder Co., Ltd.. Zoletil was purchased from France Vic Co., Ltd. Hematoxylin and eosin (HE) staining solution were purchased from Shanghai YiFan Biological Technology Co., Ltd.. CD68 antibody, CD44 antibody, MMP-9 antibody, goat anti-rabbit antibody (second antibody), and DAB kits were purchased

from Boster Biological Technology Co., Ltd. A Masson detection kit was purchased from Nanjing Jiancheng Bioengineering Institute. Salvianolic acid B and ginsenoside Rg1 were purchased from Shanghai Yousi Biotechnology Co., Ltd.. The purity of the SalB and Rg1 was more than 98% detected by HPLC (Fig. 1S, Supplementary Material). Unless otherwise noted, reagents were purchased from Sinopharm Chemical Reagent Co., Ltd.

Establishment of PE model and SalB/Rg1 treatment

To confirm the establishment of the PE model by 45 μm microspheres successfully, rats were randomly divided into 2 groups: pulmonary embolism group (PE, $n=10$) and Control group (Control, $n=10$). Rats of from the PE group were injected with one million polystyrene microspheres/kg intravenously once a week for three consecutive weeks. Rats in the Control group were given the same volume of saline at the same time.

After we confirmed that 45 μm microspheres were suitable to induce PE, we evaluated the effects of SalB/Rg1 against PE. The rats were randomly divided into 3 groups: Control group (Control, $n=10$), pulmonary embolism group (PE, $n=10$), and SalB/Rg1 group (SalB/Rg1, $n=7$). Rats from the PE and SalB/Rg1 groups were injected with one million polystyrene microspheres/kg intravenously once a week for four consecutive weeks to induce PE, while the rats in control group were injected with saline at the same time. Then, rats from the Control and PE groups were administered an intraperitoneal injection of saline for four weeks, while rats from the SalB/Rg1 group were administrated an intraperitoneal injection of 20 mg/kg of SalB/Rg1 for four weeks after the second injection of microspheres.

Heart rate (HR) measurement

Rats were weighed and anesthetized with 30 mg/kg of zoletil then fixed on the experimental table. The electrodes were placed subcutaneously into the limbs. According to the connection mode of left upper limb red, left lower limb green, and right lower limb black. The HR of the rats was measured and analyzed using PowerLab software (AD Instruments, Australia).

Organ index and ventricular hypertrophy index assessment

After measurement of HR, the rats were euthanized with a lethal dose of 200 mg/kg of pentobarbital. The organs were weighed and tibial length was measured. The left or right pulmonary index was calculated as the ratio of left or right pulmonary weight to body weight. The myocardial hypertrophy index was calculated by the ratio of heart weight to tibial length

(HW/TL). The ratio of right heart weight to left heart plus septum weight (RH/(LH+S)) were also assessed for ventricular hypertrophy.

Hematoxylin and eosin (H&E) staining

The fresh lung samples and right ventricle samples were fixed in 10% neutral-buffered paraformaldehyde for 48 hours and then were paraffin-embedded. 5 mm slices were cut for histopathological examination. After the slices were dewaxed and hydrated, they were stained with hematoxylin solution for 15 mins, differentiated with 1% alcohol hydrochloric acid for 2-3 seconds, then rinsed in distilled water. Next the slices were stained with eosin solution for 5 mins followed by dehydration with graded alcohol and clearing in xylene. Photomicrographs were taken using an Olympus BX51 microscope plus an Olympus DP71 CCD camera (Olympus, Tokyo, Japan).

The quantification of microspheres was based on H&E staining. There were a large number of smooth spherical vacuoles in the lung samples of the PE rats. The spherical vacuoles were identified as microspheres based on their diameter of about 45 μm . Eight visual fields were randomly obtained, and microspheres were counted according to the 8 fields. The average number of microspheres in the 8 fields was calculated for each rat.

The lung interstitium was stained purple in the H&E staining. The purple interstitial area of lung was quantified by Image-Pro Plus 6.0 software. The mean value of 8 fields per sample was calculated for every rat. The quantification of cardiomyocyte cross-sectional area (CCSA) was based on H&E staining. The 3 fields of per right ventricle sample were captured and 10 CCSA were quantified for per fields using Image-Pro Plus 6.0 software. The mean of CCSA in 3 fields was calculated for every rat.

Masson staining

Deparaffinized lung slices were stained with nuclear dyeing liquid for 1 min, washed with flushing fluid for 30 seconds, stained with plasma dyeing liquid for 1 min, washed with flushing fluid for 30 seconds, stained with color separation fluid for about 8 mins, drained and stained with counter dyeing liquid for about 5 mins, and washed with absolute alcohol. Photomicrographs were taken using an Olympus BX51 microscope plus an Olympus DP71 CCD camera (Olympus, Tokyo, Japan).

Immunohistochemical staining

Antigen was retrieved for paraffin-embedded slices in sodium citrate buffer (pH 6.0) for 20 mins using a microwave oven. After incubating with 3% H_2O_2 for 30 mins, the slices were rinsed with water and incubated with the primary antibody (CD68, CD44, or

MMP-9 antibody diluted 1:100 in 1% PBS) overnight at 4°C. Then, the slices were rinsed and incubated with the goat anti-rabbit antibody for 1 h at 37°C, then stained by DAB kit and hematoxylin. Photomicrographs were taken using an Olympus BX51 microscope plus an Olympus DP71 CCD camera (Olympus, Tokyo, Japan). The quantification of the positive staining area and integrated optical density (IOD) were based on Image-Pro Plus 6.0 software. Five images from each rat were analyzed and IOD/positive area was calculated to express the mean staining intensity.

Statistical analysis

Statistical analysis was performed using GraphPad Prism 5.0 (GraphPad software, LA Jolla, CA, USA). Multiple-group comparisons were made using a one-way ANOVA test and data were performed with Bonferroni correction. A Student's t-test (two-tailed, paired) was used for two-group comparisons. All data were expressed as mean \pm standard error, $p < 0.05$ was statistically significant.

Results

First the PE model induced by 45 μm microspheres was set up. As shown in Fig. 1a, the right pulmonary index (RPI) of the PE group was higher in comparison with the Control group (3.64 ± 0.47 vs. 2.34 ± 0.40 mg/g, $p < 0.001$), while the left pulmonary index (LPI) showed an increasing tendency in the PE group (Fig. 1b). Because the increase of RPI was more obvious than LPI, the histochemical observation of right lung tissues based on H&E staining was conducted, and the different appearance between alveoli and microspheres was in evidence. The shapes of alveoli were irregular, while the microspheres were round and smooth (Fig. 1c). The number of microspheres (25.77 ± 4.94 per field) was counted based on being round, smooth, and about 45 μm in size (Fig. 1d). RV hypertrophy is another important parameter during the development and progression of PE, and an increased tendency of RH/(LH+S) and HW/TL in the PE group was observed compared with the Control group (Fig. 1e,f). The representative pictures of H&E stain for RV were shown in Fig. 1g. The CCSA of RV was quantified per field (Fig. 1h), and the data of CCSA in the PE group was significantly higher than in the Control group (0.02 ± 0.00 vs. 0.01 ± 0.00 mm^2 , $p < 0.01$).

After we set up the PE model successfully, the protective effects of SalB/Rg1 on the lungs were evaluated according the experimental scheme shown in Fig. 2. As shown in Fig. 3a and 3b, both the RPI (2.83 ± 0.16 vs. 2.20 ± 0.19 mg/g, $p < 0.001$) and LPI (1.45 ± 0.12 vs. 1.15 ± 0.06 mg/g, $p < 0.001$) of the PE group significantly increased in comparison with the Control group, and SalB/Rg1 not only down-regulated RPI (2.60 ± 0.13 vs. 2.83 ± 0.16 mg/g, $p < 0.05$), but also

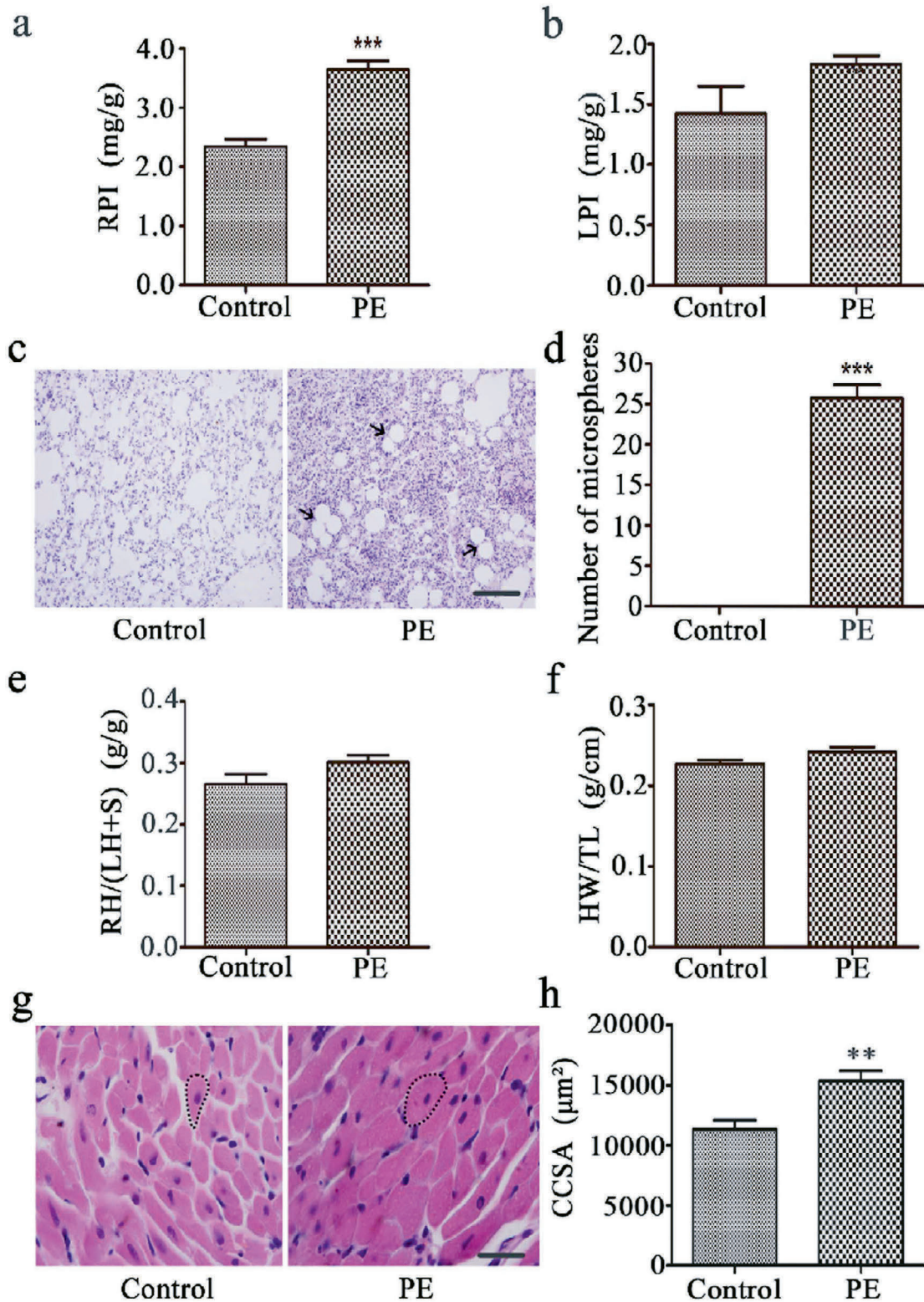


Fig. 1. The rat model of chronic PE induced by 45 μm polystyrene microspheres. a. The effect of polystyrene microspheres on the right lung index (RPI). b. The effect of polystyrene microspheres on the left lung index (LPI). c. The representative graphs of H&E staining for the right lung with the arrows indicating microspheres. Scale bar: 100 μm. d. Quantification of microsphere number according to H&E staining. e. Quantification of the weight ratio of the right heart to left heart plus septum (RH/(LH+S)). f. Quantification of the ratio of heart weight to tibial length (HW/TL). g. The representative images of H&E staining for the right ventricle, the dotted circle indicates the size of the cardiomyocytes. Scale bar: 20 μm. h. Quantification of cardiomyocyte cross-sectional area (CCSA) according to H&E staining. All the values are expressed as mean ± SE. ****p*<0.001, ***p*<0.01 versus Control. *n*=10 for every group.

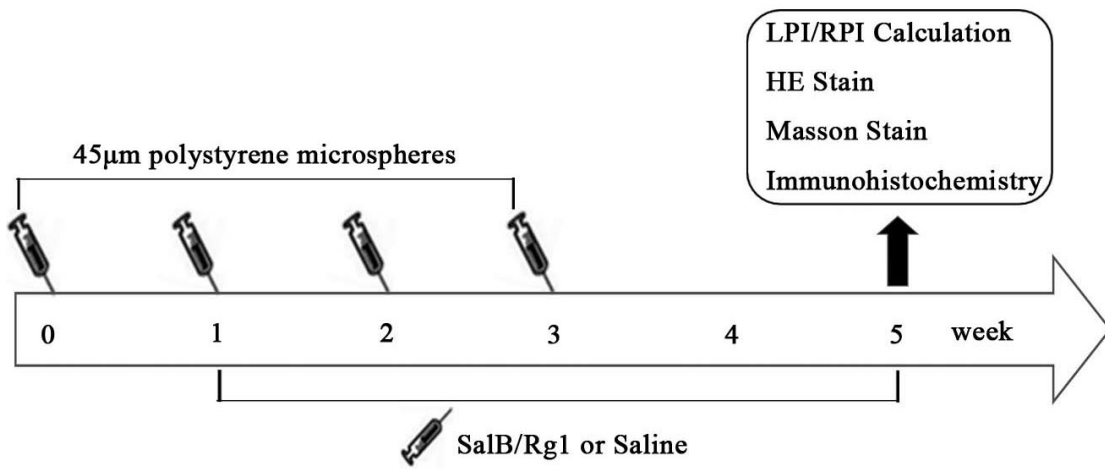


Fig. 2 The experimental scheme to evaluate the therapeutic effects of SalB/Rg1.

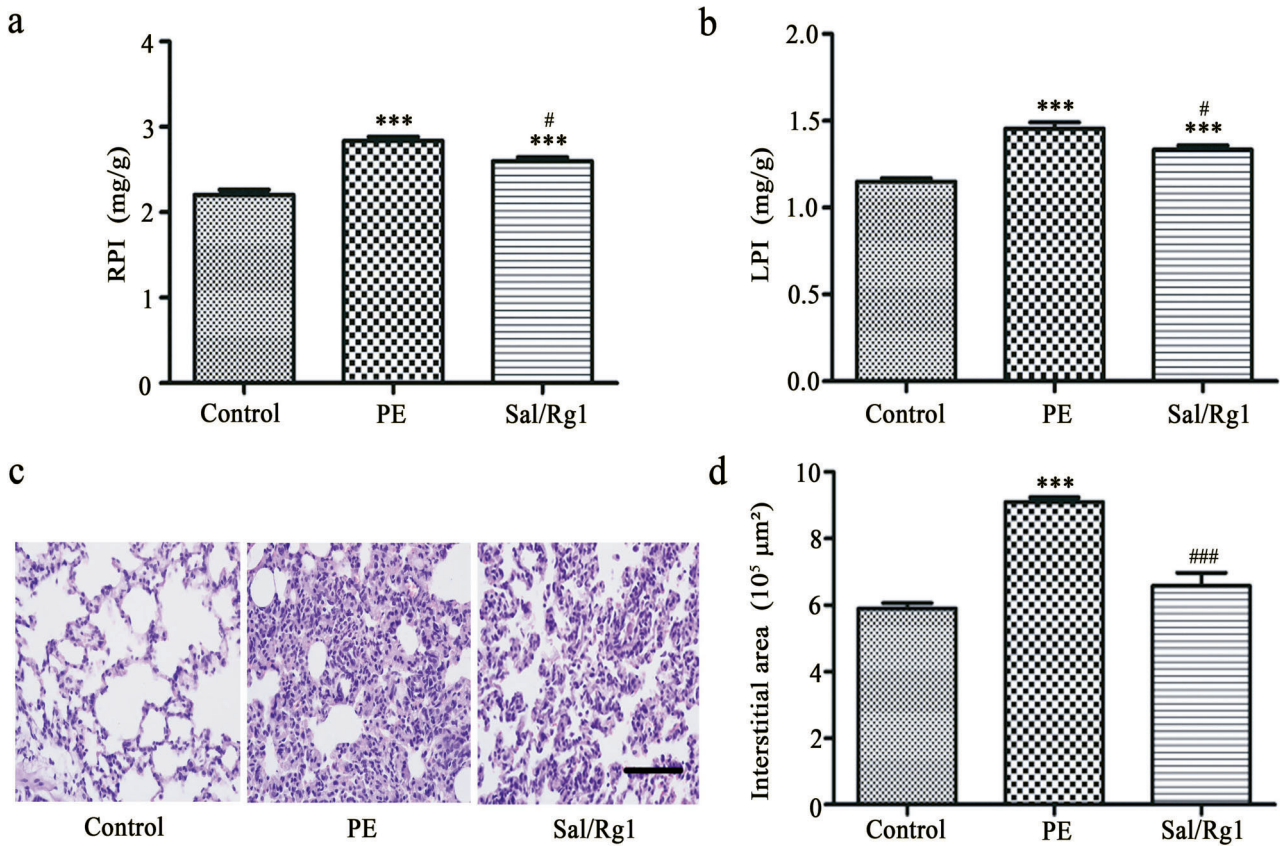


Fig. 3. SalB/Rg1 decreased the interstitial area of the lung. a. The effect of SalB/Rg1 on RPI. b. The effect of SalB/Rg1 on LPI. c. The representative graphs of the right lung interstitium in H&E staining. d. The quantification of the interstitial area. All the values are expressed as mean ± SE. ***p<0.001 versus Control, #p<0.05, ###p<0.001 versus PE. n=10 in the Control and PE groups; n=7 in the SalB/Rg1 group. Scale bar: 100 µm.

LPI (1.33 ± 0.07 vs. 1.45 ± 0.12 mg/g, $p < 0.05$) considerably. Then lung interstitial change, as another indication of PE, was observed through H&E staining. As shown in Fig. 3c, lung inflammation, thickened alveolar walls, increased lung interstitium, and decreased alveolar space were observed in the PE group compared to the Control group, and SalB/Rg1 ameliorated the interstitial structure of the lung significantly. Fig. 3d showed an increase of lung interstitial area in the PE group (0.91 ± 0.05 vs. 0.59 ± 0.05 mm², $p < 0.001$), and this increase was significantly reversed in the SalB/Rg1 group (0.66 ± 0.17 vs. 0.91 ± 0.05 mm², $p < 0.001$).

After H&E staining, inflammatory cell infiltration was also observed in the lung interstitium. The types of inflammatory cells involved and the efficiency of SalB/Rg1 were illustrated following. As two important inflammatory cells, macrophages and neutrophils were investigated through immunohistochemical staining. CD68 positive cells (macrophages) in the PE group were significantly increased compared to the Control group (0.20 ± 0.04 vs. 0.01 ± 0.01 , $p < 0.001$), while no regulation of SalB/Rg1 was found in comparison with the PE group (Fig. 4a and 4b). The immunohistochemical stain for CD44 positive cells

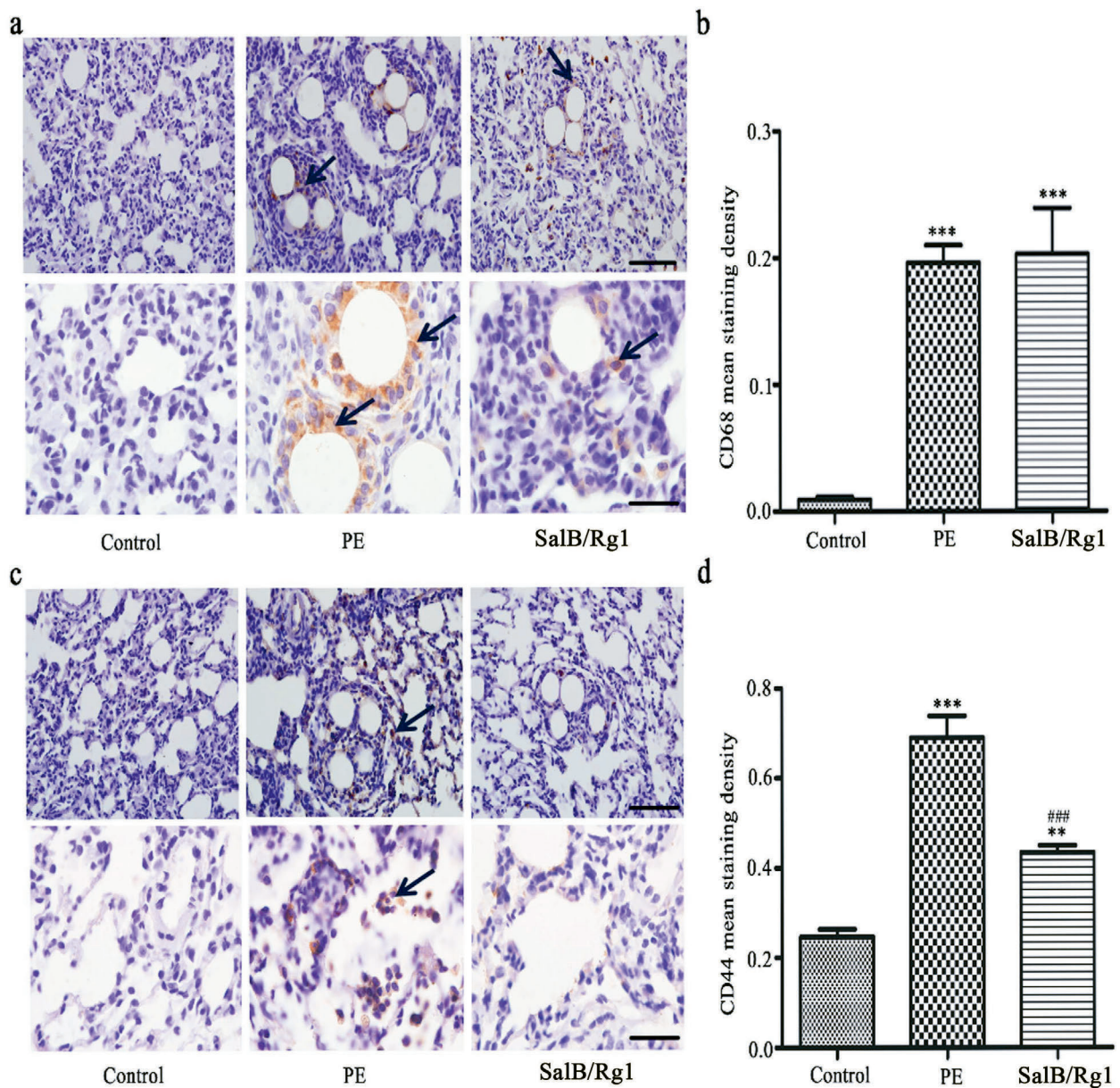


Fig. 4. SalB/Rg1 inhibited the infiltration of inflammatory cells in the right lung. a. The above images show representative CD68 immunohistochemistry staining at a low magnification (scale bar: 100 μ m) and the images below at a high magnification (scale bar: 50 μ m). The arrows represent CD68 positive cells. b. The mean staining intensity was assessed for CD68 immunohistochemistry staining. c. The above images show representative CD44 immunohistochemistry staining at low magnification (scale bar: 100 μ m) and the images below at a high magnification (scale bar: 50 μ m). The arrows represent CD44 positive cells. d. The mean staining intensity was assessed for CD44 immunohistochemistry staining. All the values are expressed as mean \pm SE. ** $p < 0.01$, *** $p < 0.001$ versus Control; ### $p < 0.001$ versus PE. $n = 10$ in the Control and PE groups. $n = 7$ in the SalB/Rg1 group.

(neutrophils) was conducted (Fig. 3c,d). The mean staining density of CD44 was up-regulated in the PE group in comparison to the Control group (0.69 ± 0.15 vs. 0.25 ± 0.05 , $p < 0.001$), and this up-regulation was inhibited by SalB/Rg1 (0.44 ± 0.04 vs. 0.69 ± 0.15 , $p < 0.001$).

Because lung inflammation affected the elasticity of alveoli and lead to pulmonary fibrosis, the impacts of SalB/Rg1 on pulmonary fibrosis were further evaluated. First, Masson staining was conducted to evaluate pulmonary fibrosis as shown in Fig. 5a. Blue

collagen fibers were profoundly increased in the PE group compared with the Control group, and SalB/Rg1 markedly ameliorated the deposition of blue collagen fibers. Then to detect whether pulmonary fibrosis was related to matrix metalloproteinase-9 (MMP-9), an immunohistochemical stain for MMP-9 was conducted. As shown in Fig. 5b, MMP-9 positive cells were significantly obvious in the PE group compared to the Control group. SalB/Rg1 treatment down-regulated MMP-9 positive cells in comparison with the PE group significantly.

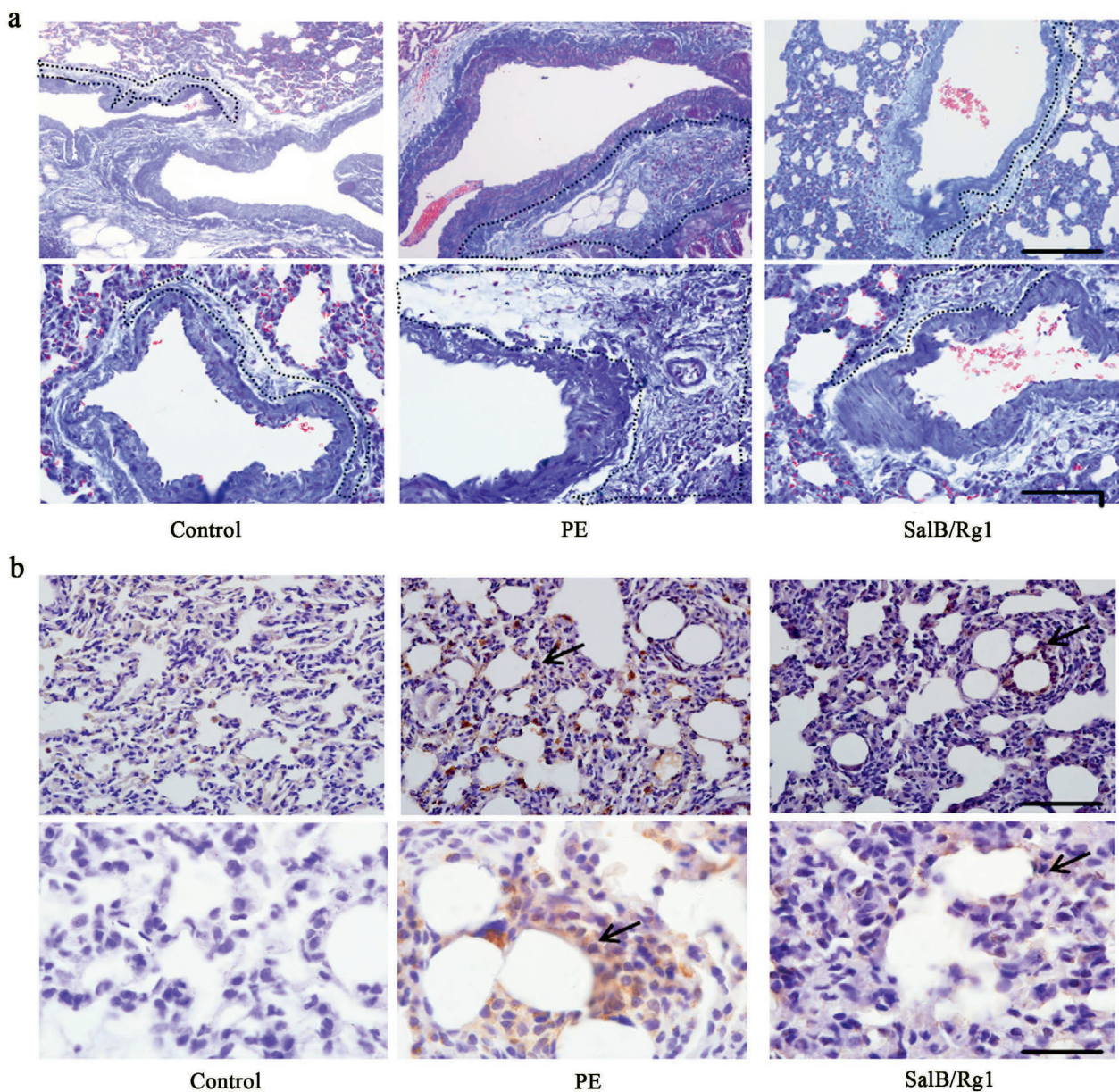


Fig. 5. SalB/Rg1 improved the pulmonary fibrosis. a. The above images show representative Masson staining at a low magnification (scale bar: 100 μ m) and the images below at a high magnification (scale bar: 50 μ m). Dotted lines mark the range of collagen fiber deposition. b. The above images show representative MMP-9 immunohistochemistry staining at a low magnification (scale bar: 100 μ m) and the images below at a high magnification (scale bar: 50 μ m). The arrows represent MMP-9 positive cells. $n=10$ in the Control and PE groups. $n=7$ in the SalB/Rg1 group.

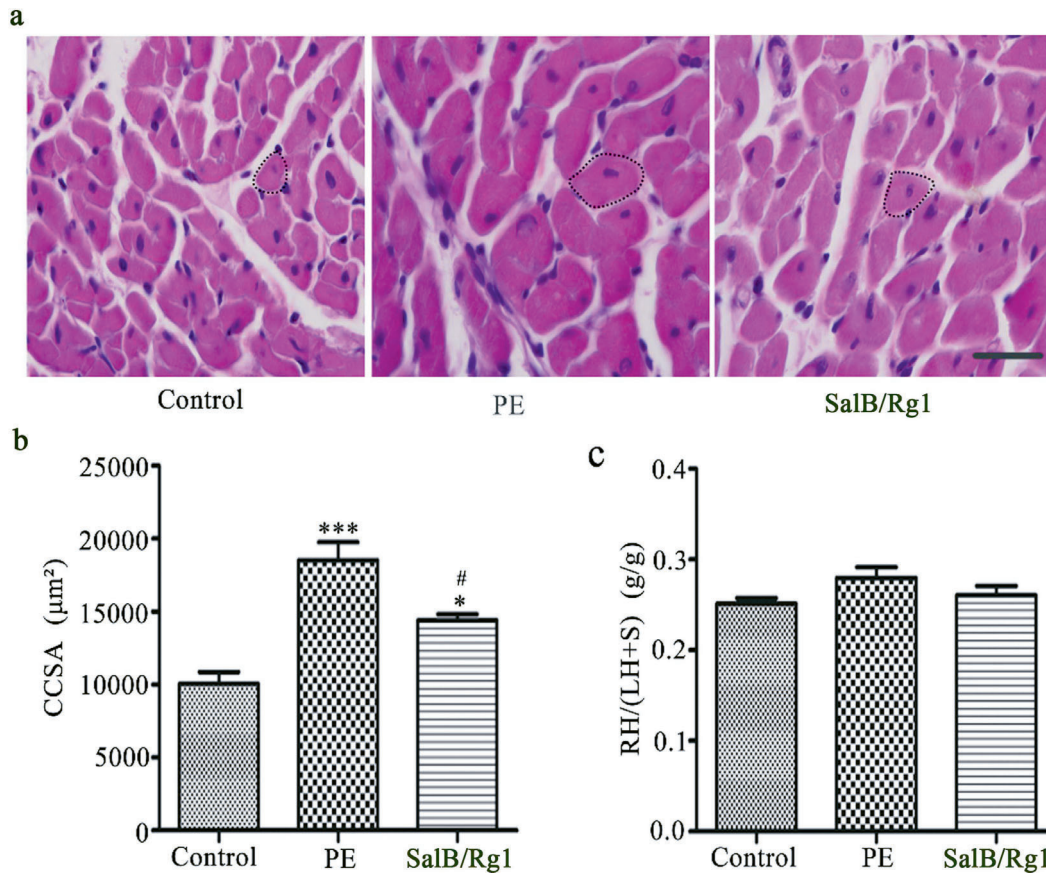


Fig. 6. SalB/Rg1 down-regulated cardiomyocyte cross-sectional area. a. The representative images of H&E staining for right ventricle, the dotted circle indicated the size of cardiomyocytes. Scale bar: 20 μm. b. Quantification of right ventricle cardiomyocyte cross-sectional area (CCSA) in H&E staining. c. Quantification of the weight ratio of right heart to left heart plus septum (RH/(LH+S)). All the values are expressed as mean ± SE. * $p < 0.05$, *** $p < 0.001$ versus Control; # $p < 0.05$, versus PE. $n = 10$ in Control and PE groups. $n = 7$ in SalB/Rg1 group.

After observation of the efficiency of SalB/Rg1 on the lung, the protective effect of SalB/Rg1 on the right heart was further investigated. PE resulted in an increase in RV cardiomyocyte size and RV hypertrophy. The representative photomicrographs of H&E staining for RV were shown in Fig. 6a. Fig. 6b showed that CCSA was significantly increased in the PE group in comparison to the Control group (0.02 ± 0.00 vs. 0.01 ± 0.00 mm², $p < 0.001$). And SalB/Rg1 significantly down-regulated CCSA compared to the PE group (0.01 ± 0.00 vs. 0.02 ± 0.00 mm², $p < 0.05$). Besides, RH/(LH+S) as an index of ventricular hypertrophy in the PE group was higher than that in the Control group. SalB/Rg1 also caused a decreasing tendency in RH/(LH+S) compared with the PE group in Fig. 6c.

Discussion

In the present study, PE was induced by 45 μm microspheres and characterized by increased LPI and RPI, enlarged lung interstitial area, aggravated in-

flammatory cell infiltration, and fibrosis on the lung, along with cardiac hypertrophy on the heart. SalB/Rg1, a combination of SalB and Rg1, exerted protective effects not only on the lung, but also on the heart in PE rats.

Multiple mechanisms have been proposed for PE, among them inflammation is a crucial player. Neutrophils are classic inflammatory cells, and their levels are tightly associated with the extent of inflammation (TOBA *et al.* 2016). Neutrophils infiltrate the venous thrombus early and trigger a cascade of inflammatory reactions that can destroy surrounding tissues, facilitate micro thrombosis, and result in PE (PUJHARI *et al.* 2020). In our research, SalB/Rg1 attenuated the infiltration of neutrophils and suppressed pulmonary interstitial changes.

Matrix metalloproteinases (MMPs) have been viewed as a promising target in the search for cardiovascular disease applications (BAGGIO *et al.* 2020). Previous studies in our laboratory have shown that SalB functioned as a competitive inhibitor of MMP-9 and efficiently prevented cardiac remodeling, which

was consistent with the present finding in PE (JIANG *et al.* 2010). The effect of MMP-9 deficiency was elucidated on deep venous thrombosis. MMP-9 modulated midterm vein wall collagen content, with a local inflammatory and pro-fibrotic environment (MUKHOPADHYAY *et al.* 2019). MMP-12 was also a valid target for pharmacological intervention, its inhibitor has significant therapeutic potential for the chronic obstructive pulmonary disease (MAGNUSSEN *et al.* 2011). In the current study, the protective effects of SalB/Rg1 on pulmonary inflammation and fibrosis may be correlated to its inhibition of MMP-9 activity. The inhibition of SalB/Rg1 on other MMPs remains to be further investigated.

Chronic increase in pulmonary vascular resistance translates into elevated RV afterload during the development and progression of PE. To cope with the increased afterload, RV undergoes structural and functional changes, which ultimately causes RV dilatation and failure (STAM *et al.* 2019). RV hypertrophy is an abnormal enlargement or pathologic increase in muscle mass of the RV in response to pressure overload, most commonly due to severe lung disease. PE is a major source of morbidity and mortality, patient outcome depends on how well the RV can sustain the increased afterload caused by the embolic burden. In the present study, RV hypertrophy was attenuated by SalB/Rg1. This finding is consistent with our previous report that SalB/Rg1 prevented or delayed the progression of cardiac remodeling, ameliorated cardiac structure and function.

In summary, we have shown that SalB/Rg1 significantly improved PE induced by microspheres for the first time. SalB/Rg1 not only ameliorated the pulmonary changes of early PE, but also held the prevention on RV hypertrophy of post-PE, indicating the potential of SalB/Rg1 for further development.

Acknowledgments

This work was supported by the Inter-governmental Science and Technology Innovation Cooperation Program, Ministry of Science and Technology of China (No. 2021YFE0111300), National Natural Science Foundation of China (81770478, 81970395), Shanghai Science and Technology Development Foundation (21S21901900) and Biological Resources Program, Chinese Academy of Sciences (KFJ-BRP-008-005).

Author Contributions

Research concept and design: H.B., H.N.; Collection and/or assembly of data: L.W., X.W.; Data analysis and interpretation: H.B., H.N.; Writing of the article: H.B., K.C., J.Y.; Critical revision of the article: H.B., L.W., K.C.; Final approval of article: J.Y., B.J.

Conflict of Interest

The authors declare no conflict of interest associated with this manuscript.

Supplementary Material

Supplementary Material to this article can be found online at:

<http://www.isez.pan.krakow.pl/en/fovia-biologica.html>

References

- BAGGIO C., VELAZQUEZ J.V., FRAGAI M., NORDGREN T.M., PELLECCIA M. 2020. Therapeutic Targeting of MMP-12 for the Treatment of Chronic Obstructive Pulmonary Disease. *J. Med. Chem.* **63**: 12911-12920. <https://doi.org/10.1021/acs.jmedchem.0c01285>
- BAO S., ZOU Y., WANG B., LI Y., ZHU J., LUO Y., LI J. 2015. Ginsenoside Rg1 improves lipopolysaccharide-induced acute lung injury by inhibiting inflammatory responses and modulating infiltration of M2 macrophages. *Int. Immunopharmacol.* **28**: 429-434. <https://doi.org/10.1016/j.intimp.2015.06.022>
- BARCO S., SCHMIDTMANN I., AGENO W., BAUERSACHS R.M., BECATTINI C., BERNARDI E., BEYER-WESTENDORF J., BONACCINI L., BRACHMANN J., CHRIST M., CZIHAL M., DUERSCHMIED D., EMPEN K., ESPINOLA-KLEIN C., FONSECA J.H., FICKER C., GENTH-ZOTZ S., JIMÉNEZ D., HARJOLA V.P., HELD M., PRAT L IOGNA., LANGE T.J., MANOLIS A., MEYER A., MUSTONEN P., RAUCH-KROEHNERT U., RUIZ-ARTACHO P., SCHELLONG S., SCHWAIBLMAIR M., STAHLBERG R., WESTERWEELE P.E. 2020. Early discharge and home treatment of patients with low-risk pulmonary embolism with the oral factor Xa inhibitor rivaroxaban: an international multicentre single-arm clinical trial. *Eur. Heart J.* **41**: 509-518. <https://doi.org/10.1093/eurheartj/ehz367>
- BRESSER P., FEDULLO P.F., AUGER W.R., CHANNICK R.N., ROBBINS I.M., KERR K.M., JAMIESON S.W., RUBIN L.J. 2004. Continuous intravenous epoprostenol for chronic thromboembolic pulmonary hypertension. *Eur. Respir. J.* **23**: 595-600. <https://doi.org/10.1183/09031936.04.00020004>
- DENG Y., YANG M., XU F., ZHANG Q., ZHAO Q., YU H., LI D., ZHANG G., LU A., CHO K., TENG F., WU P., WANG L., WU W., LIU X., GUO D., JIANG B. 2015a. Combined Salvianolic Acid B and Ginsenoside Rg1 Exerts Cardioprotection against Ischemia/Reperfusion Injury in Rats. *Plos One* **10**: e0135435. <https://doi.org/10.1371/journal.pone.0135435>
- DENG Y.P., ZHANG T.T., TENG F.K., LI D.F., XU F., CHO K.K., XU J.H., YIN J., ZHANG L., LIU Q., YANG M., WU W.Y., LIU X., GUO D.A., JIANG B.H. 2015b. Ginsenoside Rg1 and Rb1, in combination with salvianolic acid B, play different roles in myocardial infarction in rats. *J. Chin. Med. Assoc.* **78**: 114-120. <https://doi.org/10.1016/j.jcma.2014.10.001>
- JIANG B.H., CHEN J., XU L., GAO Z., DENG Y., WANG Y., XU F., SHEN X., GUO D.A. 2010. Salvianolic acid B functioned as a competitive inhibitor of matrix metalloproteinase-9 and efficiently prevented cardiac remodeling. *BMC Pharmacol* **10**. <https://doi.org/10.1186/1471-2210-10-10>
- KONSTANTINIDES S.V., MEYER G., BECATTINI C., BUENO H., GEERSING G.-J., HARJOLA V.-P., HUISMAN M.V., HUMBERT M., JENNINGS C.S., JIMÉNEZ D., KUCHER N., LANG I.M., LANKEIT M., LORUSSO R., MAZZOLAI L., MENEVEAU N., NÍ AINLE.F., PRANDONI P., PRUSZCZYK P., RIGHINI M., TORBICKI A., VAN BELLE E., ZAMORANO J.L., GALIÉ N., GIBBS J.S.R., ABOYANS V., AGENO W., S. AGEWALL, A.G. ALMEIDA, F. ANDREOTTI, E. BARBATO, J. BAUERSACHS, A. BAUMBACH, F. BEYGUI, J. CARLSEN, M. DE CARLO,

- M. DELCROIX, V. DELGADO, P.E. SUBIAS, D. FITZSIMONS, S. GAINE, S.Z. GOLDBERGER, D. GOPALAN, G. HABIB, S. HALVORSEN, D. JENKINS, H.A. KATUS, B. KJELLSTRÖM, M. LAINSCAK, P. LANCELOTTI, G. LEE, G. LE GAL, E. MESSAS, J. MORAIS, S.E. PETERSEN, A.S. PETRONIO, M.F. PIEPOLI, S. PRICE, M. ROFFI, A. SALVI, O. SANCHEZ, E. SHLYAKHTO, I.A. SIMPSON, S. STORTECKY, M. THIELMANN, A.V. NOORDEGRAAF, C. BECATTINI, H. BUENO, G.-J. GEERSING, V.-P. HARJOLA, M.V. HUISMAN, M. HUMBERT, C.S. JENNINGS, D. JIMÉNEZ, N. KUCHER, I.M. LANG, M. ŁANKĘT, R. LORUSSO, L. MAZZOLAI, N. MENEVEAU, F. NÍ AINLE, P. PRANDONI, P. PRUSZCZYK, M. RIGHINI, A. TORBICKI, E. VANBELLE, J. LUISZAMORANO, S. WINDECKER, V. ABOYANS, C. BAIGENT, J.-P. COLLET, V. DEAN, V. DELGADO, D. FITZSIMONS, C.P. GALE, D. GROBBEE, S. HALVORSEN, G. HINDRICKS, B. IUNG, P. JÜNI, H.A. KATUS, U. LANDMESSER, C. LECLERCQ, M. LETTINO, B.S. LEWIS, B. MERKELY, C. MUELLER, S.E. PETERSEN, A. SONIA PETRONIO, D.J. RICHTER, M. ROFFI, E. SHLYAKHTO, I.A. SIMPSON, M. SOUSA-UVA, R.M. TOUYZ, N. HAMMOUDI, H. HAYRAPETYAN, J. MASCHERBAUER, F. IBRAHIMOV, O. POLONETSKY, P. LANCELOTTI, M. TOKMAKOVA, B. SKORIC, I. MICHALOLIAKOS, M. HUTYRA, S. MELLEMKJAER, M. MOSTAFA, J. REINMETS, P. JÄÄSKELÄINEN, D. ANGOULVANT, J. BAUERSACHS, G. GIANNAKOULAS, E. ZIMA, C.D. VIZZA, A. SUGRALIYEV, I. BYTYÇI, A. MACA, E. EREMINIENE, S. HUIJNEN, R. XUEREB, N. DIACONU, N. BULATOVIC, I. ASFALOU, M. BOSEVSKI, S. HALVORSEN, B. SOBKOWICZ, D. FERREIRA, A.O. PETRIS, O. MOISEEVA, M. ZAVATTA, S. OBRADOVIC, I. ŠIMKOVA, P. RADSEL, B. IBANEZ, G. WIKSTRÖM, D. AUJESKY, C. KAYMAZ, PARKHOMENKO A. PEPKE-ZABA J. 2019. 2019 ESC Guidelines for the diagnosis and management of acute pulmonary embolism developed in collaboration with the European Respiratory Society (ERS). *Eur. Heart J.* **41**: 543-603. <https://doi.org/10.1183/13993003.01647-2019>
- MAGNUSSEN H., WATZ H., KIRSTEN A., WANG M., WRAY H., SAMUELSSON V., MOJ., KAY R. 2011. Safety and tolerability of an oral MMP-9 and -12 inhibitor, AZD1236, in patients with moderate-to-severe COPD: a randomised controlled 6-week trial. *Pulm. Pharmacol. Ther.* **24**: 563-70. <https://doi.org/10.1016/j.pupt.2011.05.003>
- MUKHOPADHYAY S., JOHNSON T.A., DURU N., BUZZA M.S., PAWARN.R., SARKAR R., ANTALIST.M. 2019. Fibrinolysis and Inflammation in Venous Thrombus Resolution. *Front Immunol.* **10**: 1348. <https://doi.org/10.3389/fimmu.2019.01348>
- NETO-NEVES E.M., BROWN M.B., ZARETSKAIA M.V., REZANIA S., GOODWILL A.G., MCCARTHY B.P., PERSOHN S.A., TERRITO P.R., KLINE J.A. 2017. Chronic Embolic Pulmonary Hypertension Caused by Pulmonary Embolism and Vascular Endothelial Growth Factor Inhibition. *Am. J. Pathol.* **187**: 700-712. <https://doi.org/10.1016/j.ajpath.2016.12.004>
- PUJHARI S., PAUL S., AHLUWALIA J., RASGON J.L. 2020. Clotting disorder in severe acute respiratory syndrome coronavirus 2. *Rev. Med. Virol.* undefined: e2177. <https://doi.org/10.1002/rmv.2177>
- QIAO Z., XU Y. 2016. Salvianolic Acid B Alleviating Myocardium Injury In Ischemia Reperfusion Rats. *Afr. J. Tradit. Complement Altern. Med.* **13**:157-161. <https://doi.org/10.21010/ajtcam.v13i4.20>
- STAM K., CAI Z., VAN DER VELDE N., VAN DUIN R., LAM E., VAN DER VELDEN J., HIRSCH A., DUNCKER D.J., MERKUS D. 2019. Cardiac remodelling in a swine model of chronic thromboembolic pulmonary hypertension: comparison of right vs. left ventricle. *J. Physiol.* **597**: 4465-4480. <https://doi.org/10.1113/JP277896>
- TOBA H., CANNON P.L., YABLUCHANSKIY A., IYER R.P., D'ARMIENTO J., LINDSEY M.L. Transgenic overexpression of macrophage matrix metalloproteinase-9 exacerbates age-related cardiac hypertrophy, vessel rarefaction, inflammation, and fibrosis. 2016. *Am. J. Physiol. Heart Circ. Physiol.* **312**: H375-H383. <https://doi.org/10.1152/ajpheart.00633.2016>
- TOBA M., NAGAOKA T., MORIO Y., SATO K., UCHIDA K., HOMMA N., TAKAHASHI K. Involvement of Rho kinase in the pathogenesis of acute pulmonary embolism-induced polystyrene microspheres in rats. 2008. *Am. J. Physiol-Lung C.* **298**: L297-L303. <https://doi.org/10.1152/ajplung.90237.2008>
- WENDELBOE A.M., RASKOB G.E. 2016. Global Burden of Thrombosis: Epidemiologic Aspects. *Circ. Res.* **118**: 1340-7. <https://doi.org/10.1161/CIRCRESAHA.115.306841>
- YANG Y., LIU B., TAYLOR J., HUANG Z., GUPTA S., THUMMA S., WU L., WANG S., EVERETT G. 2020. Prevalence and Clinical Impact of Atrial Fibrillation in Patients with Pulmonary Embolism. *South Med. J.* **113**: 93-97. <https://doi.org/10.14423/SMJ.0000000000001059>
- ZHAO Q., YANG M., DENG Y., YU H., WANG L., TENG F., CHO K., MA H., WU P., LI X., WU W., LIU X., XU F., JIANG B., GUO D.A. 2015. The Safety Evaluation of Salvianolic Acid B and Ginsenoside Rg1 Combination on Mice. *Int. J. Mol. Sci.* **16**: 29345-56. <https://doi.org/10.3390/ijms161226176>